THE PHOTOGRAMMETRIC RECORD

The Photogrammetric Record 29(148): 383–401 (December 2014)
DOI: 10.1111/phor.12078

FULLY AUTOMATIC GENERATION OF GEOINFORMATION PRODUCTS WITH CHINESE ZY-3 SATELLITE IMAGERY

YONGJUN ZHANG (zhangyj@whu.edu.cn)
BO WANG (461306789@qq.com)
ZUXUN ZHANG (zhangzx@cae.cn)
YANSONG DUAN (ysduan@whu.edu.cn)
YONG ZHANG (6553961@qq.com)
MINGWEI SUN (mingweis@qq.com)
SHUNPING JI (jishunping2000@163.com)

School of Remote Sensing and Information Engineering, Wuhan University, P.R. China

Abstract

The advantages of continuously and soundly obtaining large multidimensional, multiscale and multitemporal observation datasets from satellite remote sensing make it indispensable in building a national spatial data infrastructure. This paper introduces the ZY-3 satellite developed in China and discusses a fully automatic data-processing system to generate geoinformation products, such as digital elevation models (DEMs) and digital orthophotomaps (DOMs), based on ZY-3 imagery. The key technologies of automatic geoinformation product generation, including strip image-based bundle adjustment together with creating DEMs and DOMs, are illustrated. The accuracies of the georeferencing and automatically generated geoinformation products are also discussed. This automatic data-processing system is shown to provide a good foundation for near real-time derivation of such geoinformation products and for the promotion and application of Chinese domestic satellites.

KEYWORDS: automatic data processing, digital elevation model, digital orthophotomap, geoinformation products, ZY-3 satellite imagery

INTRODUCTION

DIGITAL ELEVATION MODELS (DEMs) and digital orthophotomaps (DOMs) are important sources of geographical information produced by photogrammetry and remote sensing (Mantovani et al., 1996; Zomer et al., 2002; Nichol et al., 2006). These products are widely used in resources investigations (Durga et al., 2009), environmental monitoring (Stowe et al., 1997) and mapping applications (Cihlar, 2000).

Basic theories and pioneer programmes of satellite remote sensing have been useful since 1962 when the satellite programme called CORONA was implemented (Galiatsatos et al., 2008). Over the past few decades, many great achievements have taken place in satellite remote sensing technology. IKONOS is well known for its success in mapping agricultural and urban areas (Helmholz and Rottensteiner, 2009; Bhaskaran et al., 2010); its pan-sharpened imagery has a 1 m ground resolution. QuickBird is also used in mapping and geomorphology (Siart et al., 2009). The most pertinent satellite imagery in the USA is produced by GeoEye (Norris, 2011), which receives, and is expected to continue to receive, two-thirds of its revenues from the US government. An advanced automatic data-processing system has been developed by the Centre National d'Études Spatiales (CNES) for the SPOT series of satellite imagery (Davranche et al., 2009). In recent years, satellite remote sensing has seen many spurts in its development. The US satellite WorldView-2, which can achieve a spatial resolution of 0·41 m and has eight image bands, still maintains a leading advantage. Israel's EROS-B can obtain 0·7 m spatial resolution in its high-quality images because of its TDI (time delay and integration) charge-coupled devices (CCDs). The French Pleiades system also produces images with 0·7 m spatial resolution, with stereo-images in the same strip produced by a cyclical swing every 25 s (roll: 60°, pitch: 60°) (Flamanc and Maillet, 2005). In addition, the availability of other high-resolution satellite data from a range of space programmes initiated by different countries also provides exciting opportunities for earth observation.

Based on the above background, there are three key technologies for generating fundamental geographical information products such as DEMs and DOMs with satellite data:

(1) *Geometric orientation technology*. Bundle block adjustment with satellite images, also known as spatio-triangulation, which was first developed and tested with SPOT across-track stereo-images (Rochon and Toutin, 1986), is usually used for geometric orientation. To achieve high-accuracy orientation results, satellite photogrammetry generally uses ground control points (GCPs) in a single scene for image data orientation (Fraser and Yamakawa, 2004). To achieve a more stable orientation result in sparse control areas such as seas and forests, spatio-triangulation based on strip images is adopted (a single strip image typically covers about 50 km by 4000 km on the earth's surface). Because rational polynomial coefficients (RPCs) (Noguchi et al., 2004; Fraser et al., 2006) are convenient and widely used in processing satellite data, this paper also makes a free transition from rigorous collinearity equations to RPCs to optimise the efficiency of processing after a bundle adjustment.
(2) *Intensive image-matching technology*. Such matching between multi-view images can acquire a large number of photogrammetric matching point clouds (Zhang and Gruen, 2004; 2006). DEM products can be generated under the assistance of the public geographical reference data, such as from the Shuttle Radar Topography Mission (SRTM).
(3) *Seamless stitching technology*. This can be used to generate regional DOMs. To achieve seamless stitching, a least squares adjustment method that minimises both the geometric and radiometric differences among adjacent ortho-images is proposed. After least squares adjustment, the model parameters for stitching can be calculated and a seamlessly stitched DOM can be generated.

Until recently, the excessive time and cost for processing satellite remote sensing data has been a major problem. The processing techniques have lagged behind the large amounts

of data that could be acquired, and often obtaining ground control information has been too difficult at times. However, the "industrialisation" of geographical information services has become more important in the 21st century, and the great challenge to photogrammetry and remote sensing is to find faster and more accurate solutions to processing satellite imagery.

Chinese ZY-3 Satellite

China launched its domestic earth observation programme in the 1970s. Thus far, four subprogrammes have been built, which consist of meteorological, marine, environmental and land resource (ZY) satellite systems. The key strategies of the domestic satellite data-processing system, include the automation of data processing, the so-called "cyberisation" of operation services, and the intelligence of the information analysis (Tang and Cong, 2011). Several advanced data-processing systems have already realised different degrees of automatic processing (Leprince et al., 2007; Gruen, 2012), and there are many successful experiences that are worthy references (Fraser et al., 2002; Poli and Toutin, 2012). The ZY-3 satellite data-processing system applies related photogrammetric theories and algorithms and realises near real-time automatic generation of advanced surveying and mapping products, such as DEMs and DOMs. These products can greatly improve the operational service capabilities of a satellite system and set a solid foundation for the Chinese earth observation programme (Chen et al., 2002; Hu et al., 2005).

On 9th January 2012, China successfully launched the ZY-3 satellite into orbit with a Long-March rocket from the Taiyuan Satellite Launch Centre in Shanxi Province. As the first civil Chinese high-resolution remote sensing satellite capable of stereoscopic imaging, the ZY-3 satellite is planned to acquire the basic geographical information of China, as well as other parts of the world. It aims to provide steady and reliable data sources for surveying and mapping at a scale of 1:50 000, land resource surveys, geological investigations and so on. Some important parameters of the ZY-3 satellite and its cameras are shown in Table I; further information can be found in G. Zhang et al. (2014) and Y. Zhang et al. (2014).

There are four CCD mapping pushbroom cameras on board the ZY-3 satellite, consisting of three-line panchromatic cameras (nadir view, forward view and backward view) and a multispectral camera (blue, green, red and infrared bands). When the reflected light passes through the four groups of lenses of the optical unit body, it converges onto the

Table I. Important parameters of the ZY-3 satellite and its cameras.

Parameter	*Value*
Orbital altitude	505·984 km
Orbital inclination	97·421 degrees
Regression cycle	59 days
Attitude stability	5×10^{-4} degrees/s (3 sigma)
Image width	Forward view and backward view: 52·3 km
	Nadir view: 51·1 km
	Multispectral: 51·0 km
Focal length	Forward-, nadir- and backward-view cameras: 1700 mm
	Multispectral camera: 1750 mm
CCD parameters	Forward and backward views: 16 300 pixels, 3·5 m GSD, pixel size 10 μm
	Nadir view: 24 530 pixels, 2·1 m GSD, pixel size 7 μm
	Multispectral: 16 300 pixels, GSD 5·8 m, pixel size 20 μm
Quantisation value	10 bits
Intersection angles	Forward and nadir view 22·0 degrees
	Nadir and backward view 22·0 degrees

CCD devices which are in the same focal plane. The intersection angles of the forward to nadir views and the nadir to backward views are both 22·0 degrees. Consequently, stereo-images are acquired by the three cameras with large intersection angles. The ground resolution of the nadir-view camera is 2·1 m, the resolutions of the forward and backward views are both 3·5 m, and that of the multispectral camera is 5·8 m. The ZY-3 satellite is configured with a double-frequency GPS (Global Positioning System), a laser reflector, a high-accuracy star tracker, and high-precision gyroscopes for orbit positioning and orientation.

The ZY-3 satellite ground processing system follows a fully automatic data-driven workflow, which consists of two main steps, data pre-processing and geoinformation product generation. The data pre-processing system takes into account data decompression, data cataloguing and radiometric correction. The product generation system includes a set of automatic processes, such as spatio-triangulation, DEM extraction, ortho-image rectification and so on. This paper introduces the key technologies of geoinformation product generation based on the ZY-3 satellite imagery and evaluates the accuracy of the generated products.

KEY TECHNOLOGIES OF ZY-3 SATELLITE DATA PROCESSING

After data pre-processing, the developed geoinformation product generation system is automatically activated. The workflow of automatic generation of geoinformation products is shown in Fig. 1. First, the geometric modelling process is started. More precise orientation parameters can be obtained by spatio-triangulation with corresponding image points and automatically matched GCPs as well as the onboard position and orientation observations. Second, geometric rectification, DEM extraction and epipolar stereo generation were able to work in parallel based on the results of geometric modelling. The methods of geometric rectification and epipolar stereo generation have been thoroughly investigated in the literature (Baboo and Devi, 2011; Wang et al., 2011). This paper only focuses on spatio-triangulation, together with DEM and DOM product generation. In order to improve the speed of geometric calculation between image space and object space, the

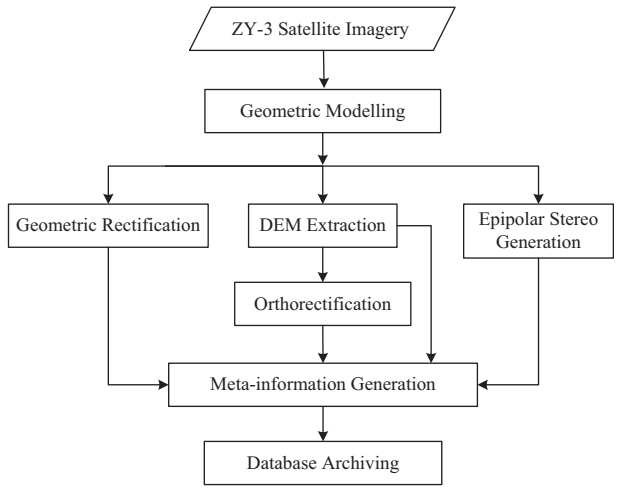

FIG. 1. Workflow of generating geoinformation products.

standard RPCs are generated with the refined attitude and orbit parameters after bundle adjustment. Dense image matching based on three-line images is conducted to extract the object coordinates of the dense points and feature lines; then a DEM is generated based on the extracted object coordinates of the dense points and feature lines. The DOM is created by orthorectification and colour fusion based on the original image, the generated DEM and precise orientation parameters. Finally, meta-information of these products is generated and all the products are uploaded to the database by database archiving.

Automatic Spatio-triangulation

Spatio-triangulation is conducted to build a rigid geometric projection between the image and space features and to obtain more precise orientation parameters for each scanner line. Based on the characteristics of the ZY-3 satellite data, spatio-triangulation with a strict geometric model of the long-strip imagery is adopted. There are several techniques in this procedure including image matching, automatic extraction of control points and bundle block adjustment.

In the image-matching step, an object-based image-matching method is adopted. It searches the point in object space in the direction of elevation with a fixed step and finds its corresponding point based on the terrain and the approximate epipolar geometry constraints (Gruen and Akca, 2005; Bellavia et al., 2008). The processing objects are long-strip ZY-3 satellite images. For example, the file size of a nadir-view image is usually about 90 gigabytes (GB), which is impossible to process on a single computer because of the time-efficiency requirement. As shown in Fig. 2, the nadir-view image is logically subdivided into many blocks, with small overlaps between adjacent blocks, to ensure there is no gap of corresponding points among adjacent blocks. In this case, these blocks can be simultaneously processed by multiple computers in parallel. Local binary pattern (LBP) and local contrast (LC) operators (Ojala et al., 2002) are used for feature-point extraction in every block of the nadir-view images. Then, by using the onboard measurement of attitude and orbit parameters, corresponding points can be predicted and matched from the forward- and backward-view images, with feature points extracted from the nadir-view images. Finally, all of the matched corresponding points are integrated together for further processing of the strip-based spatio-triangulation.

By this image-matching strategy, about 50 000 evenly distributed corresponding points, on average, are obtained from the nadir-, forward- and backward-view images since the length of a strip is usually longer than 4000 km. The GCPs are automatically extracted by matching between the nadir-view image and the available geographical information (Tao

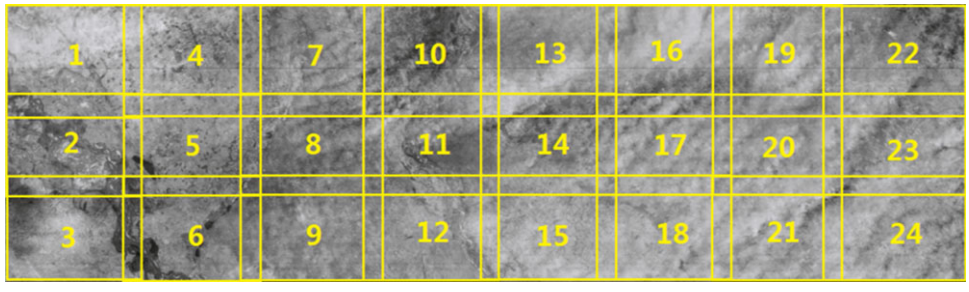

FIG. 2. Sample blocks of ZY-3 data for parallel image matching. Note the overlaps between adjacent blocks.

et al., 2011). The extracted control points from public geographical reference data (including DOMs and SRTM), or other high-accuracy terrain data, provide a significant contribution to the improvement of the absolute accuracy of ZY-3 satellite data by incorporating them into the bundle adjustment.

Unlike traditional methods that typically use RPCs to represent the geometric model in a bundle adjustment and three-dimensional information extraction, a strict geometric model of perspective projection across the satellite's track, and the near-parallel projection along its track, is used during the bundle adjustment. In the authors' model, three position parameters and three orientation parameters for each scanner line are interpolated from the onboard measurements. This strategy has the advantage of obtaining stable and similar geo-referencing accuracy within the whole strip based on sparse and unevenly distributed GCPs. In the block adjustment, both the systematic error compensation model and the orientation image model can be used to calculate precise orientation parameters with the onboard measured orientation parameters as initial values. Camera calibration parameters are also introduced into the block adjustment in order to compensate for systematic errors in camera boresight misalignment and lens distortions.

As for the systematic error compensation model, the exterior orientation parameters (Xs, Ys, Zs, φ, ω, κ) of a certain scanner line can be represented as follows:

$$\begin{aligned} Xs &= Xs_0 + a_0 + a_1 t + a_2 t^2 \quad Ys = Ys_0 + b_0 + b_1 t + b_2 t^2 \quad Zs = Zs_0 + c_0 + c_1 t + c_2 t^2 \\ \varphi &= \varphi_0 + d_0 + d_1 t + d_2 t^2 \quad \omega = \omega_0 + e_0 + e_1 t + e_2 t^2 \quad \kappa = \kappa_0 + f_0 + f_1 t + f_2 t^2 \end{aligned} \tag{1}$$

where Xs_0, Ys_0, Zs_0, φ_0, ω_0, κ_0 are position and attitude observations, a_0, a_1, …, f_2 are the polynomial coefficients of the systematic error compensation model and t is the scanning time of a certain scanner line. The second-order polynomials in equations (1) are usually sufficient to model the object-to-image geometry during the bundle adjustment of the satellite imagery data, since the attitude and track of satellites are quite stable and change smoothly while orbiting in outer space.

Automatic Generation of DEMs

The foundation of creating a DEM is the availability of elevation information for a certain interest area. Building shadows, cloud cover, water reflection, grass reflection and other poor-texture circumstances are sources of errors in image matching, which are major issues for airborne-platform images, and these errors currently can only be eliminated by manual work. Compared to airborne platforms, satellites are much higher and the ground resolutions are also significantly lower. As a result, the influence of building shadows is much weaker, which makes fully automatic processing possible. However, with cloud cover and poor-texture areas the inferiority of satellite data is particularly prominent, because it is very difficult, or even impossible, to obtain successful image-matching results. It is inevitable that there are usually some matching gaps in an object-point dataset obtained by image-matching strategies.

In order to solve the DEM-generation problem in these kinds of areas, the publicly available SRTM data is used as an alternative information source to compensate for the matching gaps, since the internal accuracy of SRTM is about 5 m within a local area (Rodríguez et al., 2006), which is commensurate with the 1:50 000 scale mapping requirements of ZY-3 imagery. The SRTM data has to be firstly co-registered with the matched object points to eliminate the systematic offsets between the two datasets. The available point cloud registration strategy is adopted to register the two datasets in this

paper (Rabbani et al., 2007). After registration, the computed systematic offsets are added onto the SRTM data to get improved height information. The improved SRTM data has two benefits on the DEM generation from the ZY-3 satellite: the first is that it can be used to detect and remove huge blunders in dense image matching; the second benefit is that the matching gaps can be filled by the improved height information to generate reasonable DEM products.

For the convenience of parallel processing, RPCs are calculated based on the orientation parameters of each scanner line (Zhang et al., 2012) before generating a DEM. The automatic extraction of a DEM primarily involves the following four steps:

(1) The point and linear features are first extracted from the satellite images. An improved Harris operator and Hough extractor are used to extract dense features, such as lines and points.
(2) Intensive object lines and points are generated by dense image matching using the generic sensor model represented by RPCs. Fig. 3 shows the three-dimensional line features obtained by dense image matching in a mountainous region.
(3) Registration and fusion between SRTM and the obtained object points are performed to remove large blunders and compensate matching gaps caused by clouds, water bodies and so on.
(4) The DEM is obtained by removing the gross errors of image matching and interpolating these discrete object points into regular grids.

Automatic Generation of Digital Orthophotomaps

The original images acquired by satellite sensors have the characteristics of a central projection along the direction of the CCD sensor and near-parallel projection along the orbit, which definitely introduces terrain distortions when the image sensor is not pointing directly at the nadir location of the sensor. To decrease the distortion and recover the original surface, the process of orthorectification is necessary to produce a DOM. A DOM has the advantage of

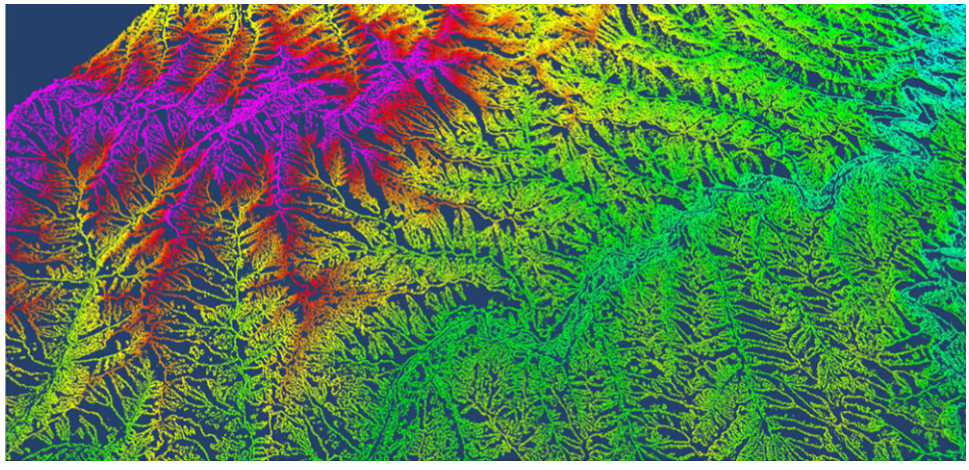

FIG. 3. Dense matching results of feature lines in a mountainous region. Different colours represent different elevations.

simultaneously sustaining spectral and plane coordinate information, which is widely used in land surveying, resource investigation, municipal planning and so on.

The purpose of the ZY-3 satellite is to produce regional geographical information products at 1:50 000 scale. Seamless stitching of several ortho-images generated from both the same strip and different strips, together with the automatic fusion of panchromatic images and multispectral images (Schetselaar, 1998), are the main topics that need to be addressed to generate satisfactory DOM products. Using the geometric orientation results of strip spatio-triangulation and DEMs to rectify the original images can ensure seamless stitching and fusion of ortho-images within the same strip. However, there are usually gaps of a few pixels between ortho-images generated from adjacent strips because each is processed independently. To stitch the ortho-images from different strips together, a least squares adjustment method that minimises both the geometric and radiometric differences between adjacent ortho-images is proposed to calculate the stitching parameters.

The proposed DOM stitching method includes five steps:

(1) Image matching based on feature points is performed to find corresponding points between adjacent ortho-images. These corresponding points are the observations in the least squares adjustment.
(2) The stitching model parameters between two adjacent ortho-images, which include six affine transformation parameters for geometric consistency, are calculated by the corresponding points, as shown as follows:

$$\begin{aligned} x_2 &= a_0 + a_1 x_1 + a_2 y_1 \\ y_2 &= b_0 + b_1 x_1 + b_2 y_1 \end{aligned} \tag{2}$$

where a_0, b_0, a_1, b_1, a_2, b_2 are the affine transformation parameters between two adjacent ortho-images and x_1, y_1, x_2, y_2 are the coordinates of a corresponding point pair in image space.

(3) During the least squares adjustment process for geometric correction, one of the ortho-images in a block should be treated as errorless in geometry to avoid a rank-defect problem in the normal equations. Suppose there are nine adjacent ortho-images within a block, and the geometric position of the ortho-image at the centre is fixed, the number of unknowns for geometric consistency is $6 \times (9 - 1) = 48$. By least squares adjustment, the 48 unknowns of the affine transformation can be solved and the geometric disparities can be minimised.
(4) For the least squares adjustment for radiometric correction, the available method proposed by Zhang et al. (2011) is used. Two linear distortion parameters are used to model the grey-value consistency of each channel of the colour image, as shown as follows:

$$g_1(x_1, y_1) = h_0 + h_1 g_2(x_2, y_2) \tag{3}$$

where h_0, h_1 are the linear distortion parameters of grey values of a certain pixel; x_1, y_1, x_2, y_2 are the coordinates of a corresponding point pair in image space; and $g_1(x_1, y_1)$, $g_2(x_2, y_2)$ are the grey values of the corresponding point pair.
(5) Finally, regional ortho-images are stitched together with the computed parameters.

Experiments and Analysis

The automatic processing system developed for ZY-3 imagery finished operational testing in May 2012. Usually one strip, longer than 4000 km, of ZY-3 satellite imagery

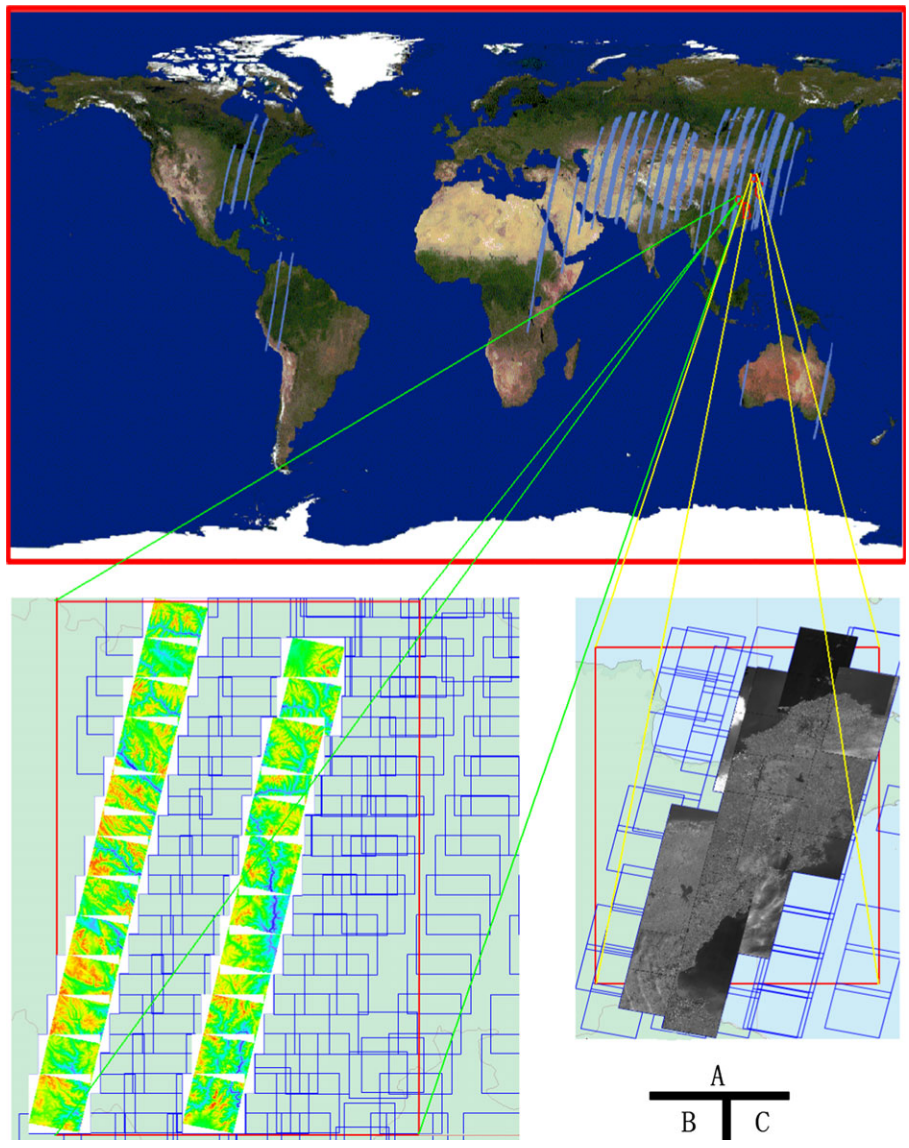

FIG. 4. Sample regional DEM and DOM products from ZY-3 satellite imagery. Top image (A): the areas (in blue) where automatically generated regional geoinformation products have been generated with the developed system up to 22nd May 2012. Bottom left (B): thumbnails of DEMs generated in Sichuan Province. Bottom right (C): thumbnails of DOMs produced in Shandong Province, China.

could be successfully processed to generate the geometric rectification, epipolar stereo, DEM and DOM products within two hours. Fig. 4(A) indicates areas where automatically generated regional geoinformation products with the developed system have been produced up to 22nd May 2012 (blue rectangles represent the ground coverage of the generated

products); Fig. 4(B) shows thumbnails of DEMs in Sichuan Province, China; and Fig. 4(C) illustrates thumbnails of DOMs in Shandong Province, China. Detailed accuracies of georeferencing and the generated DEM and DOM products will be discussed in the following sections.

Experimental Data Introduction

ZY-3 satellite images of two orbits were selected to test the accuracy of the geoinformation products to be analysed. The first dataset was acquired on 3rd February 2012 from orbit No. 381 over the calibration field of Songshan, Henan Province, China. The second dataset was acquired on 26th January 2012 from orbit No. 259 over an area of Zhejiang Province, China.

Several kinds of geographical data, including global public geographical reference data (such as MapWorld, Google Earth and SRTM), 1:10 000 scale DEMs and DOMs, and high-accuracy GCPs in the Songshan calibration field, were used as references to verify the accuracy of the generated geoinformation products.

Accuracy Evaluation for Orientation of Three-line Images

The accuracy of direct georeferencing by the onboard orientation and position parameters is shown in Table II. There are 198 check points in the Songshan area and 62 check points in the Zhejiang area. As can be seen, the planimetric accuracy, in terms of root mean square (RMS) error, was of the order of 15 m. The height accuracy was at the 30 m level, which was definitely not acceptable. Moreover, there were significant systematic shifts between the ground truth of the check points and their computed coordinates by direct georeferencing.

A bundle adjustment was performed using the automatically matched corresponding points and the control points from the global public geographical reference data. The accuracy statistics by using the high-precision points as check points (198 in Songshan; 62 in Zhejiang) are shown in Table III. It is clear that both the planimetric and the height accuracies were significantly improved by two to three times, which was due to the contribution of the public geographical data and the bundle adjustment. However, some systematic shifts still remained between the ground truth and the computed coordinates of check points using the bundle adjustment because of the limited accuracy of public geographical reference data.

Once the block adjustment was performed with field control points (three control points were used during bundle adjustment in the Songshan test data) and 1:10 000 scale DEMs and DOMs (10 control points were used during the bundle adjustment in the Zhejiang test

TABLE II. Accuracy of direct georeferencing with onboard observations.

Location	*RMS of image point residuals (pixel)*		*Max. residual of image points (pixel)*		*RMS of check point residuals (m)*		*Max. residual of check points (m)*	
	x	*y*	*x*	*y*	*Planimetry*	*Height*	*Planimetry*	*Height*
Songshan	0·571	0·549	1·485	1·411	13·906	34·920	21·715	41·931
Zhejiang	0·522	0·685	2·456	2·496	7·032	24·024	13·684	45·191

TABLE III. Accuracy of georeferencing after block adjustment with public geographical reference data.

Location	*RMS of image point residuals (pixel)*		*Max. residual of image points (pixel)*		*RMS of check point residuals (m)*		*Max. residual of check points (m)*	
	x	*y*	*x*	*y*	*Planimetry*	*Height*	*Planimetry*	*Height*
Songshan	0·736	0·653	2·691	2·004	7·483	11·752	12·133	13·554
Zhejiang	0·670	0·722	2·038	2·693	2·112	13·441	5·966	24·061

data), the accuracy of the bundle adjustment could be significantly improved. The accuracy of georeferencing is shown in Table IV, again using 198 check points in the Songshan area and 62 check points in Zhejiang. The planimetric accuracies of the two testfields were improved to 1·5 m, and the height accuracies were 1·6 m for Songshan and 6·7 m for Zhejiang. As can be seen from the heighting accuracy of the Zhejiang testfield, the DEM used for the height control information was not fully compatible with the stereo-imagery because objects above the terrain, such as buildings and trees, were removed from the DEM but remained in the stereo-imagery.

Accuracy Evaluation of DEMs and DOMs

Based on the Chinese national standard of 1:50 000 scale topographic mapping by photogrammetry, the accuracy requirements of a DEM are 3·0, 5·0, 8·0 and 14·0 m for flat, hilly, mountainous and highly mountainous areas, respectively, while the accuracy requirement of a DOM is 25·0 m.

Accuracy of Generated DEMs and DOMs based on Public Geographical Reference Data

The global public geographical reference data were adopted as control information during the bundle block adjustment. High-precision check points were used to evaluate the accuracy of the generated DEMs and DOMs. The accuracy statistics for the DEMs and DOMs in different terrain are shown in Table V. There are 164 check points in the mountainous area of Songshan data and 34 check points in the flat area of Songshan data. In the experiment using Zhejiang data, the number of check points is 34 in the mountainous area and 28 in the flat area. *Planimetry X*, *Planimetry Y* and *Planimetry (XY)* describe the accuracy of the DOM, and *Height* describes the accuracy of the DEM. RMS is the root mean square error of the planar and height residuals; *Mean*, *Max*. and *Min.* are the average, maximum and minimum residuals, respectively.

TABLE IV. Accuracy of georeferencing after block adjustment with accurate control points.

Location	*RMS of image point residuals (pixel)*		*Max. residual of image points (pixel)*		*RMS of check point residuals (m)*		*Max. residual of check points (m)*	
	x	*y*	*x*	*y*	*Planimetry*	*Height*	*Planimetry*	*Height*
Songshan	0·273	0·312	0·841	0·999	1·437	1·614	4·540	4·026
Zhejiang	0·522	0·684	2·463	2·452	1·453	6·676	4·891	12·356

TABLE V. Accuracy of DEM and DOM products based on public geographical reference data (m).

Terrain	*Statistics*	*Planimetry X*	*Planimetry Y*	*Planimetry (XY)*	*Height*
Mountainous area in Songshan	RMS	5·222	3·366	6·108	5·442
	Mean	−2·932	−2·069	5·685	4·348
	Max.	6·383	5·650	10·536	14·299
	Min.	−10·512	−6·337	0·622	−3·883
Flat area in Songshan	RMS	2·783	2·681	3·394	7·058
	Mean	−1·693	1·018	3·580	6·830
	Max.	3·773	6·166	6·527	9·956
	Min.	−5·147	−2·408	1·207	3·243
Mountainous area in Zhejiang	RMS	5·835	3·471	6·789	14·518
	Mean	3·606	0·018	6·075	−14·110
	Max.	11·741	6·753	11·757	−9·664
	Min.	−4·839	−10·100	1·036	−22·499
Flat area in Zhejiang	RMS	3·587	3·423	4·887	5·771
	Mean	2·662	0·736	4·477	−5·436
	Max.	9·304	6·279	10·694	−1·156
	Min.	−2·642	−6·566	0·420	−10·379

As can be seen, the accuracy of the DEMs and DOMs was limited by the accuracy of the global open geographical reference data. In the Songshan area, the planimetric accuracy was quite acceptable. The height accuracy in the mountainous area was higher than that in the flat area because too many man-made structures as well as trees existed in the latter, which apparently influenced the accuracy of the DEM. Furthermore, the value of the height RMS was almost equal to that of the height mean, which meant the geographical reference data itself contained a certain systematic error. In the Zhejiang area, the horizontal accuracy of the DOM was quite acceptable. In this mountainous area of southern China, lush forests made the terrain too complicated to assist accurate terrain recognition, which also influenced the accuracy of the DEM.

As a whole, after conducting block adjustment with the global open geographical reference data, the accuracy of the DEM was close to the national standard at 1:50 000 scale, while the accuracy of the DOM was much higher than the specified requirement.

TABLE VI. Accuracy of DEM and DOM products based on 1:10 000 scale geographical information (m).

Terrain	*Statistics*	*Planimetry X*	*Planimetry Y*	*Planimetry (XY)*	*Height*
Urban areas	RMS	2·532	2·015	3·149	4·927
	Mean	2·107	1·933	2·963	2·427
	Max.	3·951	3·070	6·207	6·323
	Min.	−0·868	−1·608	1·751	−5·450
Flat areas	RMS	1·209	1·388	2·105	3·487
	Mean	1·589	1·284	1·993	−0·241
	Max.	2·412	2·472	3·164	4·284
	Min.	−0·901	−1·022	1·118	−4·277
Mountainous areas	RMS	2·378	3·095	3·821	5·878
	Mean	2·017	3·197	3·349	1·875
	Max.	5·622	6·653	8·710	6·950
	Min.	−1·337	−1·436	0·790	−6·136

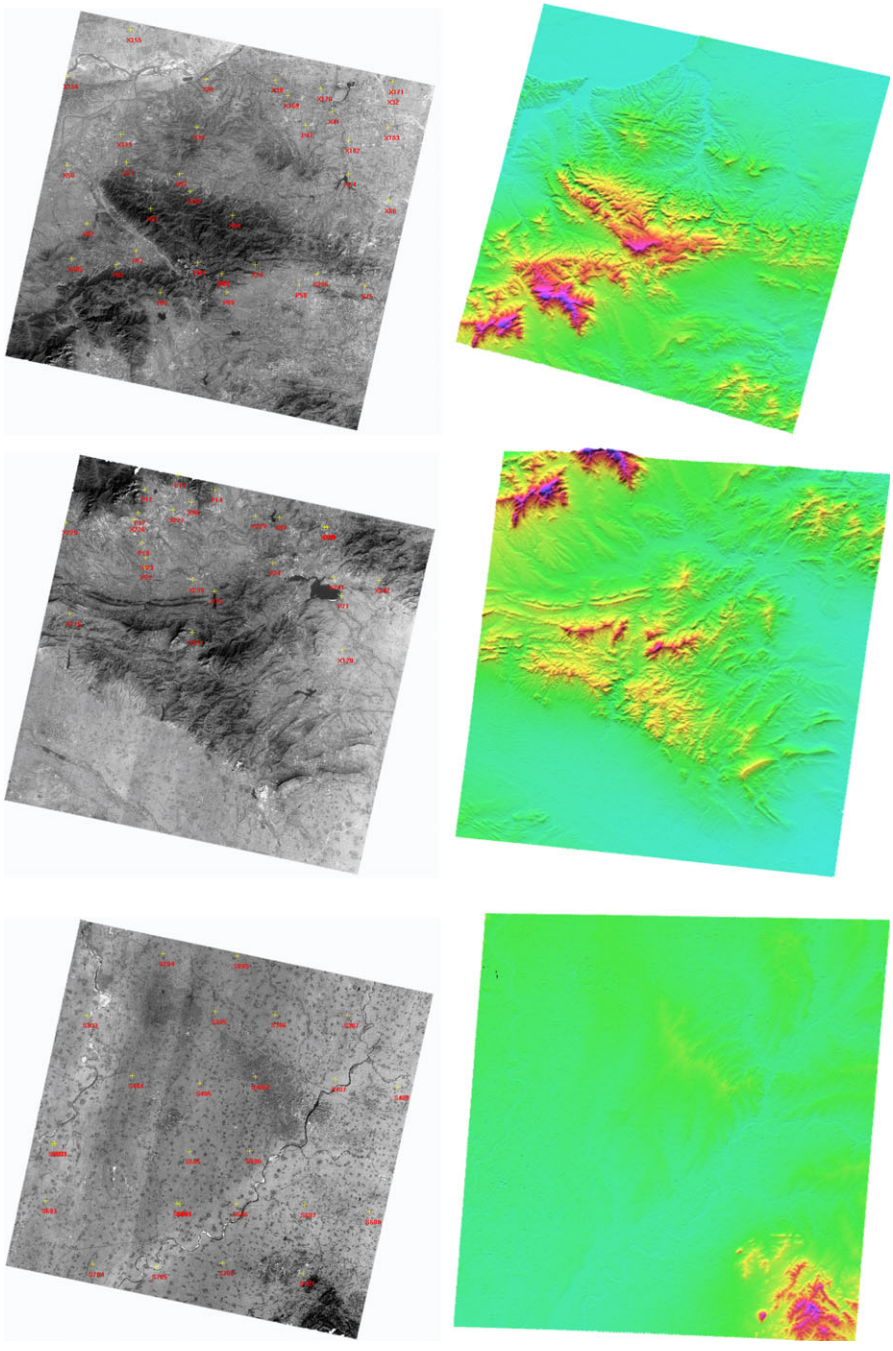

FIG. 5. DOM (left) and DEM (right) thumbnails of the Songshan test area with the distribution of check points shown in red on the DOMs. Top: mountainous terrain. Middle: hilly terrain. Bottom: flat terrain.

There were still some remaining systematic errors in the generated products because of the limited accuracy of the global public reference data.

Accuracy of DEMs and DOMs based on 1:10 000 Geographical Information

In the practical work, the basic geographical information data at 1:10 000 scale could be used in a bundle adjustment once higher accuracy was required. After extracting control points from the 1:10 000 scale DEMs and DOMs, bundle adjustment and geoinformation product generation were performed once again in the Zhejiang test area. The accuracy statistics of the generated DEMs and DOMs is shown in Table VI. In this experiment, there are 68 control points and 20 check points in urban areas, 20 and 15 in flat areas, and 48 and 17 in mountainous areas, respectively.

It can be seen from Table V that the average achievable accuracy of the DOM was 3 to 5 m. In the flat areas, the accuracy was even higher than 3 m, which verified the effectiveness of the overall adjustment method with the whole strip data. Meanwhile, after using the control points derived from the geographical information at 1:10 000 scale, the accuracy of the DEM was remarkably improved. These results also demonstrated that the quality of the product was highly dependent on the accuracy of the control points. Therefore, if more precise control points are available, the accuracy of the products could also be expected to increase.

Accuracy of Generated DEMs and DOMs based on High-accuracy GCPs

In high-accuracy mapping applications, precise ground points that are usually acquired from field measurement could be used as GCPs in the bundle adjustment. To fully evaluate the mapping potential of the ZY-3 satellite, bundle adjustment and geoinformation product generation were performed once again in the Songshan test area with 83 high-accuracy GCPs. In this experiment, three control points were used during the bundle adjustment and the other 80 ground points were used as check points to verify the accuracies of the DEM and DOM products. Fig. 5 illustrates the products of the Songshan area. The check points, which are displayed as red marks on the DOM thumbnails, are uniformly distributed on the three scenes with different terrain types. The accuracy statistics are shown in Table VII.

TABLE VII. Accuracy of DEM and DOM products based on high-accuracy GCPs (m).

Terrain	*Statistics*	*Planimetry X*	*Planimetry Y*	*Planimetry (XY)*	*Height*
Mountainous area in Songshan	RMS	2·614	1·699	3·118	3·304
	Mean	−1·028	−0·832	2·750	−0·160
	Max.	8·452	3·031	8·529	8·763
	Min.	−4·520	−4·413	0·373	−7·745
Hilly area in Songshan	RMS	1·868	2·119	2·220	2·689
	Mean	−0·639	−1·332	2·694	1·809
	Max.	2·578	3·007	4·657	5·503
	Min.	−4·091	−3·519	1·195	−2·957
Flat area in Songshan	RMS	1·420	3·016	2·859	2·020
	Mean	0·873	−2·826	3·171	1·272
	Max.	3·693	−0·165	5·572	4·597
	Min.	−2·587	−5·560	0·470	−2·004

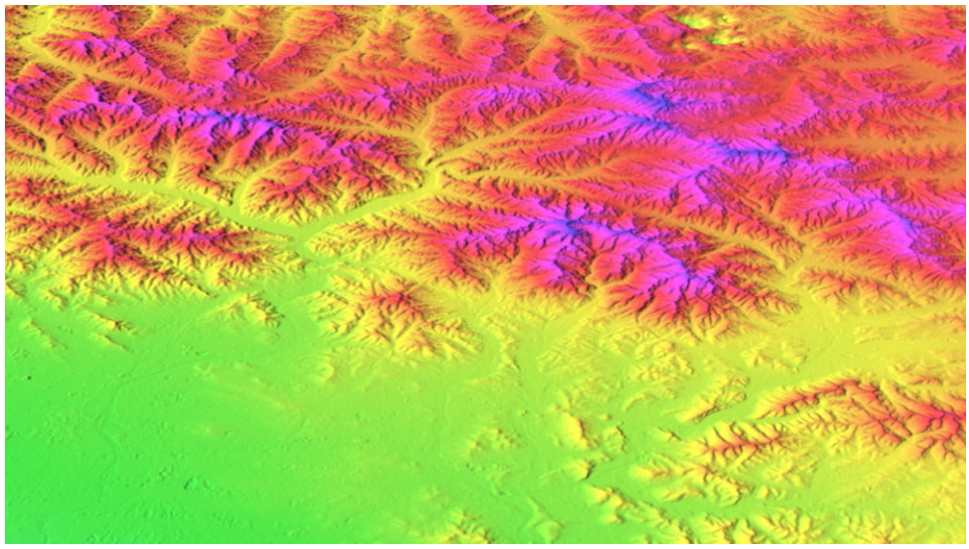

FIG. 6. Typical DEM from ZY-3 satellite imagery (Yingkou, Liaoning Province, China).

Typical DEM and DOM Products Generated from ZY-3 Satellite Imagery

The developed data-processing system was powerful for its fully automatic, near real-time processing ability. The geographical information products from the ZY-3 satellite images were also satisfactory in terms of both image quality and geometric precision. For example, Fig. 6 shows the rendered image of the DEM (25 m grid) in Yingkou in the south of Liaoning Province.

Fig. 7(a) shows a colour DOM of Dalian port, China, which illustrates the DOM quality of ZY-3 in an urban area. Fig. 6(b) depicts a colour DOM of small villages near Munich, Germany, which typifies the DOM quality in rural areas. Fig. 6(c) shows the DOM of a mountainous area in China. These high-resolution colour orthophotographs were generated by fusing the high-resolution panchromatic images with multispectral images, both of which were acquired from the ZY-3 satellite. The ground sample distance of the DOM was 2·5 m. As can be seen from Fig. 7, the visual quality of the DOMs is also very good.

CONCLUSIONS

ZY-3 is a top-quality Chinese civilian remote sensing satellite, both in its hardware configuration and the automatic processing software system which has been developed. By implementing the following five advanced algorithms of photogrammetric processing, the developed processing system can efficiently generate regional surveying and mapping products:

(1) multiple-view image matching;
(2) strip-based bundle block adjustment with systematic error compensation model;
(3) DEM generation based on multi-feature dense matching;
(4) the assistance of SRTM data; and
(5) regional DOM generation based on overall least squares matching.

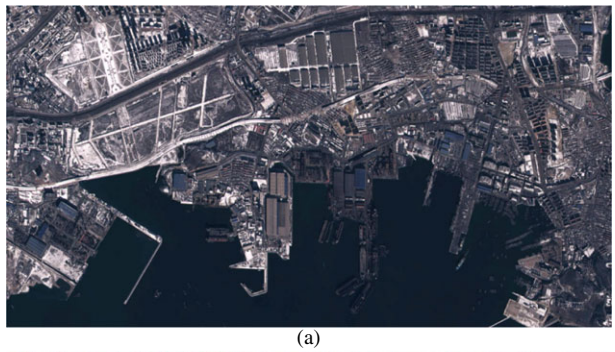

(a)

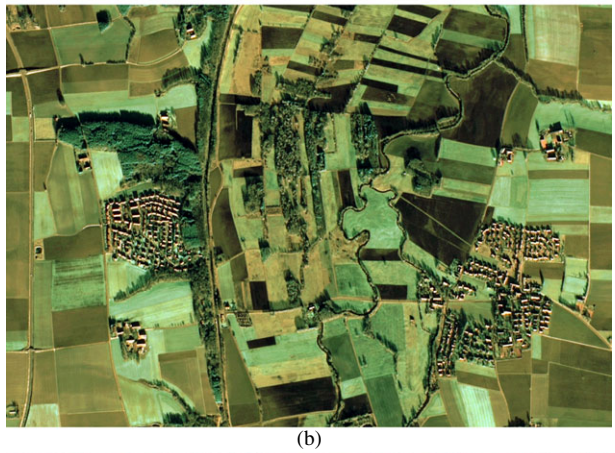

(b)

(c)

FIG. 7. Typical colour digital orthophotomap (DOM) products made from ZY-3 satellite imagery. (a) Dalian port, Liaoning Province, China. (b) A rural area near Munich, Germany. (c) A mountainous area in Jiangsu Province, China.

Bundle adjustment accuracies of about 3·5 to 7·0 m in planimetry and 5·5 to 14·0 m in height were achieved with public geographical reference data; the equivalent figures for 1:10 000 scale fundamental geographical information were 2·0 to 4·0 m in planimetry and 3·5 to 6·0 m in height. Moreover, once high-accuracy GCPs were used in the bundle adjustment, accuracies of 2·2 to 3·5 m in both planimetry and height were achieved, which

is promising for a variety of applications. The fully automatic data-processing system not only puts near real-time service of geoinformation products into operation, but also provides strong support for the promotion and applications of Chinese domestic satellites.

Acknowledgements

This work was supported in part by the National Natural Science Foundation of China with Project Nos. 41322010 and 41071233, and the National Hi-Tech Research and Development Programme with project number 2013AA12A401. Heartfelt thanks are also given for the comments and contributions of reviewers and members of the editorial team.

References

Baboo, S. S. and Devi, M. R., 2011. Geometric correction in recent high resolution satellite imagery: a case study in Coimbatore, Tamil Nadu. *International Journal of Computer Applications*, 14(1): 32–37.

Bellavia, F., Tegolo, D. and Valenti, C., 2008. A non-parametric scale-based corner detector. *Proceedings of the 19th International Conference on Pattern Recognition*, Tampa, USA. 1–4.

Bhaskaran, S., Paramananda, S. and Ramnarayan, M., 2010. Per-pixel and object-oriented classification methods for mapping urban features using Ikonos satellite data. *Applied Geography*, 30(4): 650–665.

Chen, J., Li, J., He, J. B. and Li, Z., 2002. Development of geographic information systems (GIS) in China: an overview. *Photogrammetric Engineering & Remote Sensing*, 68(4): 325–332.

Cihlar, J., 2000. Land cover mapping of large areas from satellites: status and research priorities. *International Journal of Remote Sensing*, 21(6–7): 1093–1114.

Davranche, A., Lefebvre, G. and Poulin, B., 2009. Radiometric normalization of SPOT-5 scenes: 6S atmospheric model versus pseudo-invariant features. *Photogrammetric Engineering & Remote Sensing*, 75(6): 723–728.

Durga Rao, K. H. V., Bhanumurthy, V. and Roy, P. S., 2009. Application of satellite-based rainfall products and SRTM DEM in hydrological modelling of Brahmaputra Basin. *Journal of the Indian Society of Remote Sensing*, 37(4): 587–600.

Flamanc, D. and Maillet, G., 2005. Evaluation of 3D city model production from Pleiades-HR satellite images and 2D ground maps. *International Archives of Photogrammetry, Remote Sensing and Spatial Information Sciences*, 36(8/W27). 5 pages.

Fraser, C. S., Hanley, H. B. and Yamakawa, T., 2002. Three-dimensional geopositioning accuracy of Ikonos imagery. *Photogrammetric Record*, 17(99): 465–479.

Fraser, C. S. and Yamakawa, T., 2004. Insights into the affine model for high-resolution satellite sensor orientation. *ISPRS Journal of Photogrammetry and Remote Sensing*, 58(5–6): 275–288.

Fraser, C. S., Dial, G. and Grodecki, J., 2006. Sensor orientation via RPCs. *ISPRS Journal of Photogrammetry and Remote Sensing*, 60(3): 182–194.

Galiatsatos, N., Donoghue, D. N. M. and Philip, G., 2008. High resolution elevation data derived from stereoscopic CORONA imagery with minimal ground control: an approach using Ikonos and SRTM data. *Photogrammetric Engineering & Remote Sensing*, 74(9): 1093–1106.

Gruen, A., 2012. Development and status of image matching in photogrammetry. *Photogrammetric Record*, 27(137): 36–57.

Gruen, A. and Akca, D., 2005. Least squares 3D surface and curve matching. *ISPRS Journal of Photogrammetry and Remote Sensing*, 59(3): 151–174.

Helmholz, P. and Rottensteiner, F., 2009. Automatic verification of agricultural areas using IKONOS satellite images. *International Archives of Photogrammetry, Remote Sensing and Spatial Information Sciences*, 36(1-4-7/W5). 7 pages.

Hu, X. Y., Tao, C. V. and Prenzel, B., 2005. Automatic segmentation of high-resolution satellite imagery by integrating texture, intensity, and color features. *Photogrammetric Engineering & Remote Sensing*, 71(12): 1399–1406.

Leprince, S., Barbot, S., Ayoub, F. and Avouac, J.-P., 2007. Automatic and precise orthorectification, coregistration, and subpixel correlation of satellite images: application to ground deformation measurements. *IEEE Transactions on Geoscience and Remote Sensing*, 45(6): 1529–1558.

MANTOVANI, F., SOETERS, R. and VAN WESTEN, C. J., 1996. Remote sensing techniques for landslide studies and hazard zonation in Europe. *Geomorphology*, 15(3–4): 213–225.

NICHOL, J. E., SHAKER, A. and WONG, M.-S., 2006. Application of high-resolution stereo satellite images to detailed landslide hazard assessment. *Geomorphology*, 76(1–2): 68–75.

NOGUCHI, M., FRASER, C. S., NAKAMURA, T., SHIMONO, T. and OKI, S., 2004. Accuracy assessment of QuickBird stereo imagery. *Photogrammetric Record*, 19(106): 128–137.

NORRIS, P., 2011. Developments in high resolution imaging satellites for the military. *Space Policy*, 27(1): 44–47.

OJALA, T., PIETIKAINEN, M. and MAENPAA, T., 2002. Multiresolution gray-scale and rotation invariant texture classification with local binary patterns. *IEEE Transactions on Pattern Analysis and Machine Intelligence*, 24(7): 971–987.

POLI, D. and TOUTIN, T., 2012. Review of developments in geometric modelling for high resolution satellite pushbroom sensors. *Photogrammetric Record*, 27(137): 58–73.

RABBANI, T., DIJKMAN, S., VAN DEN HEUVEL, F. and VOSSELMAN, G., 2007. An integrated approach for modelling and global registration of point clouds. *ISPRS Journal of Photogrammetry and Remote Sensing*, 61(6): 355–370.

ROCHON, G. and TOUTIN, T., 1986. SPOT – a new cartographic tool. *International Archives of Photogrammetry and Remote Sensing*, 26(4): 192–205.

RODRÍGUEZ, E., MORRIS, C. S. and BELZ, J. E., 2006. A global assessment of the SRTM performance. *Photogrammetric Engineering & Remote Sensing*, 72(3): 249–260.

SCHETSELAAR, E. M., 1998. Fusion by the IHS transform: should we use cylindrical or spherical coordinates? *International Journal of Remote Sensing*, 19(4): 759–765.

SIART, C., BUBENZER, O. and EITEL, B., 2009. Combining digital elevation data (SRTM/ASTER), high resolution satellite imagery (Quickbird) and GIS for geomorphological mapping: a multi-component case study on Mediterranean karst in Central Crete. *Geomorphology*, 112(1–2): 106–121.

STOWE, L. L., IGNATOV, A. M. and SINGH, R. R., 1997. Development, validation, and potential enhancements to the second-generation operational aerosol product at the National Environmental Satellite, Data, and Information Service of the National Oceanic and Atmospheric Administration. *Journal of Geophysical Research: Atmospheres*, 102(D14): 16923–16934.

TANG, X. M. and CONG, N., 2011. The thinking of current situation and development of Chinese mapping satellite. *Geographical Information World*, 9(2): 40–44.

TAO, P. J., LU, L. P., ZHANG, Y., ZHANG, Z. X. and ZHANG, Y. J., 2011. The automatic orientation of CBERS-02B based on existing GIS data. *Proceedings of the First Symposium on High Resolution Remote Sensing Data Processing and Applications*, Xi'an, China (on CD-ROM).

WANG, M., HU, F. and LI, J., 2011. Epipolar resampling of linear pushbroom satellite imagery by a new epipolarity model. *ISPRS Journal of Photogrammetry and Remote Sensing*, 66(3): 347–355.

ZHANG, G., JIANG, Y., LI, D., HUANG, W., PAN, H., TANG, X. and ZHU, X., 2014. In-orbit geometric calibration and validation of ZY-3 linear array sensors. *Photogrammetric Record*, 29(145): 68–88.

ZHANG, Y., ZHENG, M., XIONG, J., LU, Y. and XIONG, X., 2014. On-orbit geometric calibration of ZY-3 three-line array imagery with multistrip data sets. *IEEE Transactions on Geoscience and Remote Sensing*, 52(1, Part 1): 224–234.

ZHANG, L. and GRUEN, A., 2004. Automatic DSM generation from linear array imagery data. *International Archives of Photogrammetry, Remote Sensing and Spatial Information Sciences*, 35(B3): 128–133.

ZHANG, L. and GRUEN, A., 2006. Multi-image matching for DSM generation from IKONOS imagery. *ISPRS Journal of Photogrammetry and Remote Sensing*, 60(3): 195–211.

ZHANG, Y. J., ZHANG, Z. X., SUN, M. W. and KE, T., 2011. Precise orthoimage generation of Dunhuang wall painting. *Photogrammetric Engineering & Remote Sensing*, 77(6): 631–640.

ZHANG, Y. J., LU, Y. H., WANG, L. and HUANG, X., 2012. A new approach on optimization of the rational function model of high-resolution satellite imagery. *IEEE Transactions on Geoscience and Remote Sensing*, 50(7, Part 2): 2758–2764.

ZOMER, R., USTIN, S. and IVES, J., 2002. Using satellite remote sensing for DEM extraction in complex mountainous terrain: landscape analysis of the Makalu Barun National Park of eastern Nepal. *International Journal of Remote Sensing*, 23(1): 125–143.

Résumé

L'acquisition continue et systématique d'importants jeux de données multidimensionnelles, multiscalaires et multitemporelles au moyen de satellites d'observation rend indispensable la construction d'une infrastructure nationale de données spatiales. Cet article présente le satellite ZY-3 développé en Chine ainsi qu'un système totalement automatique de traitement de données visant à générer des produits d'information géographique tels que des modèles numériques de terrain (MNT) et des orthophotoplans numériques à partir d'images ZY-3. Les principales techniques de génération automatique de produits d'information géographique sont décrites, notamment la compensation par faisceaux sur des bandes d'images et la création des MNT et des orthophotoplans. Les précisions du géoréférencement et des produits issus du traitement automatique sont également discutées. Ce système de traitement automatique de données s'avère être une bonne base pour la fourniture en temps quasi-réel de tels produits d'information géographique ainsi que pour la promotion et l'application des satellites nationaux chinois.

Zusammenfassung

Die Vorteile einer kontinuierlichen, soliden Erfassung von großen, multi-dimensionalen, mehrskaligen und multi-temporalen Datensätzen der Satellitenfernerkundung sind unabdingbar für den Aufbau einer nationalen räumlichen Dateninfrastruktur. Dieser Beitrag stellt den chinesischen ZY-3 Satelliten vor und diskutiert ein vollautomatisches Datenprozessierungssystem für die Erzeugung von Geoinformations-Produkten, wie Digitale Höhenmodelle und Digitale Orthophotos. Die hierzu erforderlichen Schlüsseltechnologien, inclusive einer streifenbasierten Bündelausgleichung, werden beleuchtet. Ebenso werden die erzielten Genauigkeiten der Georeferenzierung und der automatisch erzeugten Geoinformations-Produkte diskutiert. Das System stellt nachweislich eine gute Basis für die nahezu in Echtzeit mögliche Ableitung von Geoinformations-Produkten dar und fördert die Anwendung chinesischer Satelliten.

Resumen

Las ventajas de obtener de forma continua y estable un gran conjunto de datos multi-escala, multidimensional y multi-temporales de teledetección por satélite hacen indispensable la construcción de una infraestructura nacional de datos espaciales. En este trabajo se presenta el satélite ZY-3 desarrollado en China y se discute un sistema totalmente automático de proceso de datos para generar productos de geoinformación, como los modelos digitales de elevación (DEM) y ortofotomapas digitales (DOM), basado en imágenes del ZY-3. Se muestran las tecnologías clave de la generación automática de productos de geoinformación, incluido el ajuste de haces basado en imágenes de barrido junto con la creación de DEMs y DOMs. También se discuten las precisiones en la georeferenciación y productos de geoinformación generados automáticamente. Este sistema automático de proceso de datos se muestra como un buen recurso para la derivar en tiempo casi real este tipo de productos de geoinformación y para la promoción y aplicación de los satélites nacionales chinos.

摘要

利用遥感卫星连续稳定地获取多维、多尺度和多时相对地观测数据,是建设国家空间基础设施的关键因素。本文介绍了中国的资源三号卫星和一套基于资源三号卫星影像的地理信息产品*(*如*DEM*和*DOM)*全自动化生产系统。自动化产品生产的关键技术包括基于条带影像的区域网平差以及*DEM*和*DOM*自动制作。论文讨论了自动化处理系统所生产地理信息产品的精度。该自动化数据处理系统可以准实时生产地理信息产品,为有效促进其他中国遥感卫星的广泛应用奠定了良好的基础。